Water vapor sources for Yangtze River Valley rainfall: Climatology, variability, and implications for rainfall forecasting

Jiangfeng Wei,[1] Paul A. Dirmeyer,[1] Michael G. Bosilovich,[2] and Renguang Wu[3]

Received 20 September 2011; revised 13 December 2011; accepted 15 December 2011; published 14 March 2012.

[1] The method of calculating water vapor flux can show the paths of moisture transport but cannot easily identify the sources and sinks of water vapor. In this study, we estimate the evaporative moisture sources for the Yangtze River Valley (YRV) rainfall with a water vapor back-trajectory method, using meteorological data from the Modern Era Retrospective-analysis for Research and Applications (MERRA). The major moisture sources and their relative contributions show large seasonal variations. The moisture from the Bay of Bengal and the western Pacific usually compensate each other both during the evolution of YRV wet season (April–September) and interannually for the wet months (peak in August). The major direct moisture sources are over YRV and its major moisture transport pathways over land, rather than over the ocean, but the ocean is important in initiating the moisture transfer. However, over these important land moisture sources, surface evapotranspiration is not controlled by soil wetness and has weak impact on the variability of rainfall. Local moisture recycling over YRV is mostly a passive response to rainfall and circulation changes. The prediction of YRV rainy season rainfall thus depends more on the knowledge of large-scale circulations and monsoons than land surface conditions.

Citation: Wei, J., P. A. Dirmeyer, M. G. Bosilovich, and R. Wu (2012), Water vapor sources for Yangtze River Valley rainfall: Climatology, variability, and implications for rainfall forecasting, *J. Geophys. Res.*, *117*, D05126, doi:10.1029/2011JD016902.

1. Introduction

[2] The Yangtze River Valley (YRV) is one of the world's most populated regions. With the longest river in Asia passing through it, this region has been threatened frequently by summer floods. For example, the flood in 1998 killed about 4,000 people and caused about $26 billion in economic losses. Floods are mostly caused by periods of heavy rainfall. Located in a monsoon region, YRV is greatly affected by the East Asian summer monsoon rainfall, which is closely connected to the patterns of water vapor transport. Every summer, the monsoon flow brings a large amount of water vapor to East China [e.g., *Huang et al.*, 2004; *Ding and Chan*, 2005]. The decadal precipitation variations over East China during the past half-century are believed to be directly related to the changes in water vapor transport [*Ding et al.*, 2008; *Huang et al.*, 1998, 2004; *Zhou et al.*, 2008; *Chen and Huang*, 2008].

[3] Figure 1 shows the dominant spatial pattern (EOF1) of the vertically integrated moisture fluxes obtained from a Principal Component Analysis (PCA) and regions where precipitation is most strongly affected by this pattern. The period of this analysis is the wet season (April–September) of YRV when the precipitation accounts for more than 70% of the annual total. The dominant pattern shows a westward flow over the tropical North Indian Ocean and a southwesterly flow that transports moisture to the middle and lower reaches of YRV. For this study, we select a rectangular area over YRV, where precipitation is strongly affected by the moisture transport, and YRV mentioned in this paper refers to this area unless otherwise stated.

[4] The basic questions we address in this study are: Where does the water vapor for YRV rainfall come from? What source regions are most important? Can we predict the rainfall using information of evaporation at the source regions? Past studies of water vapor transport over East Asia typically used bulk or kinematic methods of calculating water vapor flux, which can show the paths of transport but cannot easily identify the sources and sinks of water vapor [e.g., *Simmonds et al.*, 1999; *Zhou and Yu*, 2005; *He et al.*, 2007; *Zhou et al.*, 2008; *Zhao et al.*, 2008]. *Xu et al.* [2008] argued that the Bay of Bengal to South China Sea region is the main moisture source for the precipitation over YRV. But their conclusion is based on simple correlation analyses, so is inconclusive. Preliminary analysis of *Drumond et al.* [2011] with a Lagrangian model shows that the moisture sources for inland regions of China are mostly over land. Here we also use a Lagrangian method to track the surface evaporative moisture sources for each precipitation event over YRV and study the characteristics of

[1]Center for Ocean-Land-Atmosphere Studies, Institute of Global Environment and Society, Calverton, Maryland, USA.
[2]Global Modeling and Assimilation Office, NASA Goddard Space Flight Center, Greenbelt, Maryland, USA.
[3]Institute of Space and Earth Information Science, Chinese University of Hong Kong, Shatin, Hong Kong.

0148-0227/12/2011JD016902

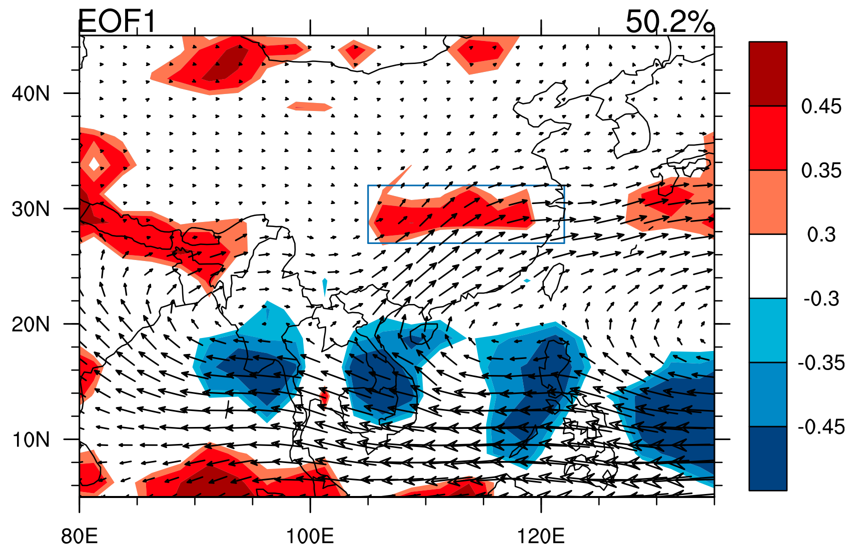

Figure 1. The first EOF (EOF1) of the 1979–2010 interannual variation of April–September average vertically integrated moisture flux (vectors) and the correlation of its corresponding first principle component time series (PC1) with precipitation at each grid point (shading). The correlations of 0.3, 0.35, and 0.45 are significant at 90%, 95%, and 99% levels, respectively. The moisture flux data is from MERRA (see section 2 for introduction) and the precipitation data is from Global Precipitation Climatology Project data set (GPCP) [*Adler et al.*, 2003]. The rectangular box is the area for further analysis.

seasonal to interannual variations of the evaporative sources. Investigation of evaporative sources over land also leads to insights into land-atmosphere interactions. The most important moisture sources are not necessarily useful for rainfall forecasts, so the potential of using the information of evaporative sources for precipitation prediction is also discussed.

2. Data and Method

[5] Observational estimates of the hydrologic cycle are still incomplete, so we need to rely on the model results or reanalysis products, although they contain various types of errors and biases [*Trenberth et al.*, 2011]. In this study, we analyze the Modern Era Retrospective-analysis for Research and Applications (MERRA) [*Rienecker et al.*, 2011]. MERRA was generated with the Goddard Earth Observing System (GEOS-5) atmospheric model and data assimilation system, with a particular emphasis on the hydrologic cycle. It is found that the global precipitation climatology and variability of MERRA are closer to observations than previous generations of reanalyses, and ocean evaporation is more realistic [*Bosilovich et al.*, 2011]. MERRA covers the period from 1979 to the present (data from 1979 through 2010 are used in this study), with a horizontal resolution of 2/3° longitude by 1/2° latitude and 72 vertical atmospheric levels.

[6] The quasi-isentropic back-trajectory (QIBT) method [*Dirmeyer and Brubaker*, 1999, 2007] is used to track the water vapor for each precipitation event (each grid with precipitation) backward in time along isentropic surfaces, assuming precipitated water is drawn from the atmospheric column in a distribution same as the specific humidity. MERRA is used to provide the meteorological data for estimating the incremental contribution of surface evapotranspiration (ET). Traces are performed on each reanalysis grid, starting from the grids with precipitation, backward in time until at least 90% of its original precipitation is attributed to ET, but no longer than 15 days (the average residence time of moisture is about 10 days). The time step for the calculation is 45 min, and the calculations and output are aggregated into pentads (5-day intervals). Please see the reference papers above for a detailed description of the QIBT method. An advantage of the QIBT method compared to using water vapor tracers in models [e.g., *Numaguti*, 1999; *Bosilovich and Schubert*, 2002] is that it can be used for post-processing and the study region can be defined after the model simulation has been finished. Several similar methods have been developed to examine the water vapor sources for precipitation [*Stohl and James*, 2004; *Sodemann et al.*, 2008].

3. Climatology

[7] Figure 2a shows the climatological time series of wet season (April–September) precipitation over YRV. The maximum rainfall is during June–July, mainly a result of the migration of the Meiyu front from south to north. Compared to the observational estimates from the Global Precipitation Climatology Project (GPCP) [*Xie et al.*, 2003] and the Climate Prediction Center Merged Analysis of Precipitation (CMAP) [*Xie and Arkin*, 1997], the rainfall in MERRA is slightly underestimated early in the rainy season and is largely overestimated afterwards. We separate the wet season into three periods according to the evolution of rainfall over YRV: April–May (before rainy season), June–July (rainy season), and August–September (after rainy season). The three periods show very different evaporative moisture sources and vertically integrated moisture fluxes (Figures 2b–2d). During April–May, before the onset of the

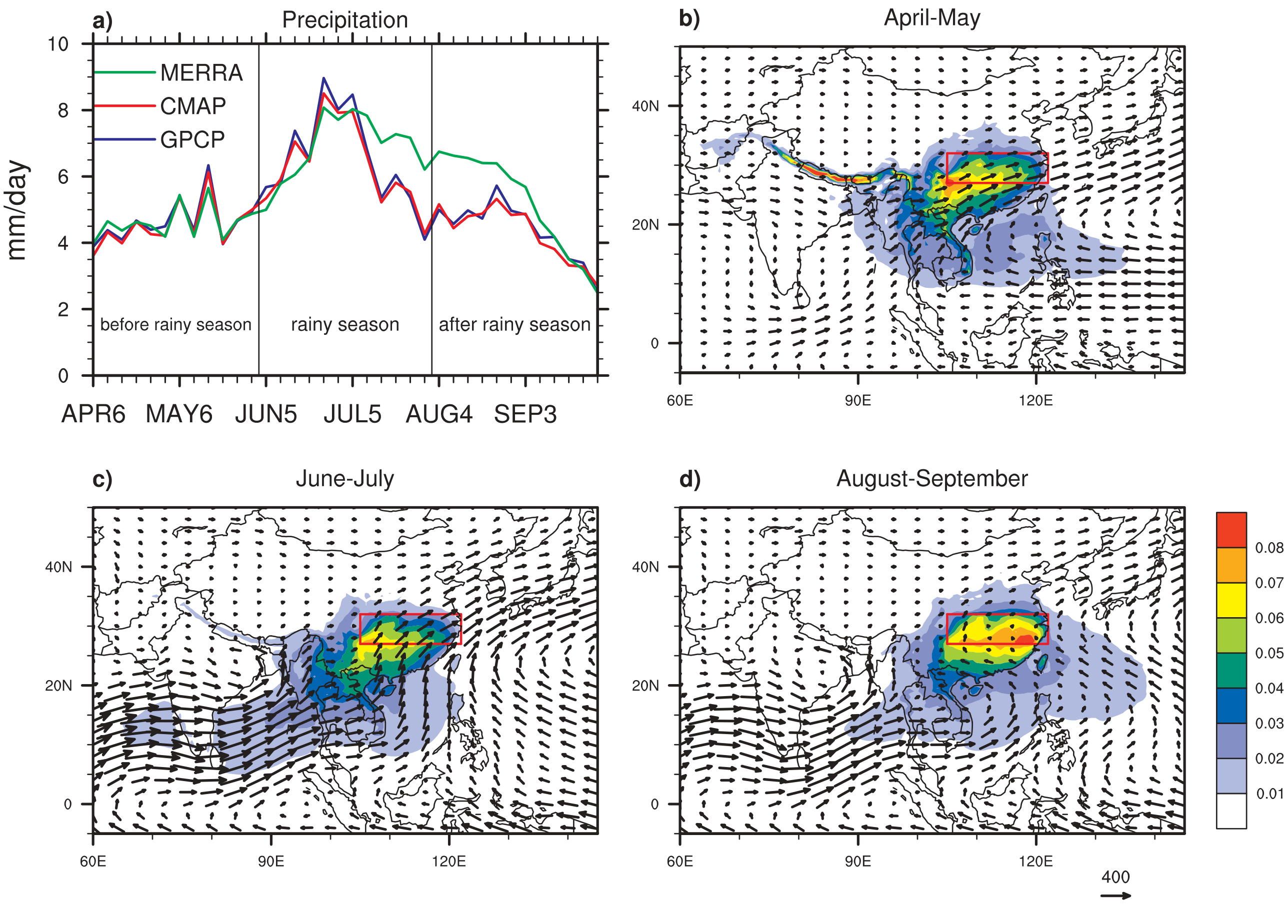

Figure 2. (a) Climatological mean pentad time series of area average precipitation over the Yangtze River Valley (YRV; rectangular box in Figure 1) from the pentad ending on April 6th to the pentad ending on October 3rd. Three data sets are shown: MERRA (1979–2010), CMAP (1979–2009), and GPCP (1979–2007). Evaporative moisture sources supplying the rainfall over YRV (red box) during (b) April–May, (c) June–July, and (d) August–September (shaded). Unit is the percentage of total rainfall over YRV (sum of all the grid points is 100). Based on MERRA data; see text for details. The arrows show the vertically integrated moisture flux (unit: kg m^{-1} s^{-1}).

East Asian monsoon the water vapor is mainly transported to YRV from the South China Sea and western Pacific. The moisture flux from the Bay of Bengal is generally too weak to directly reach YRV in large amounts, but it can indirectly reach YRV after falling as rainfall over Indochina and Southwest China and re-evaporating. During June–July, when the monsoon is strong, we can see two main branches of water vapor transport: one from the Arabian Sea and the Bay of Bengal, through Indochina and entering YRV from southwest, and the other from the South China Sea through South China and entering YRV from the south. The first branch contributes more to YRV rainfall than the second branch. During August–September, with the weakening of the East Asian monsoon the moisture is transported to YRV from all three major ocean regions: the western Pacific, the South China Sea, and the Bay of Bengal.

[8] In order to clearly show the time evolution of the evaporative contribution from major sources to YRV rainfall, we select some major moisture source regions (Figure 3a). Three land regions and three ocean regions are defined, where evaporated moisture contributes about 70% of the total YRV rainfall. Although the bias in MERRA rainfall is not expected to have a great impact on the estimated large-scale features of moisture sources, it can impact the time evolutions of evaporative contributions (Figure 3b), which is directly related to the time evolution of rainfall. In order to balance the total evaporative contributions and the observed precipitation, we make a first order calibration by scaling the evaporative contribution time series with the ratio of GPCP to MERRA rainfall over YRV at each pentad. The calibrated estimates are shown in Figure 3b. The contribution of most regions follows the time evolution of YRV rainfall, except that the contribution from the western Pacific is small during the rainy season but increases and becomes a major source after that. This is probably related to the movement of the western Pacific subtropical high and the landfall of typhoons (more discussion later) [*Ren et al.*, 2002]. The local evaporative contribution from YRV also has a larger value after the rainy season, which is related to the change of monsoon flow and the wet land surface over YRV (more discussion later). Figure 3c shows the percentage contributions of the moisture sources to YRV rainfall. The percentage contribution from YRV evaporation is actually the local recycling ratio, which is defined as the

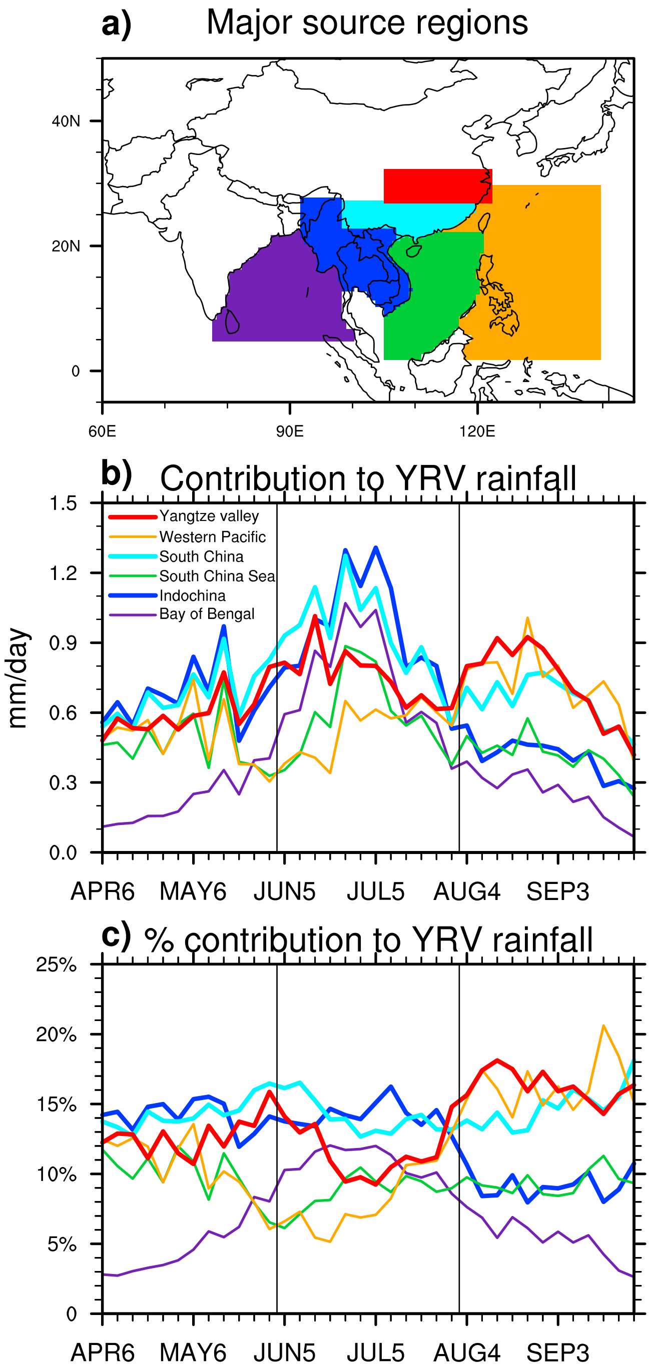

Figure 3. (a) Selected major water vapor source regions for YRV precipitation. (b) Mean pentad evolution of the evaporative contribution of different source regions in Figure 3a to the rainfall over YRV. (c) Same as Figure 3b but for the percentage contributions. The line colors in Figures 3b and 3c correspond to the mask colors in Figure 3a. The lines for the three land regions are thicker than those for the three ocean regions. The values in Figure 3b are calibrated to account for the bias in MERRA precipitation (see text).

percentage of precipitation over an area that originates as ET from the same area. The recycling ratio of YRV is lower during the rainy season. The contributions from the Bay of Bengal and western Pacific show an obvious seesaw relationship, with the contribution of the South China Sea in between.

[9] It can be seen in both Figures 2 and 3 that in most cases the land regions have higher evaporative contributions to YRV rainfall than the ocean regions, consistent with the results of *Drumond et al.* [2011]. This is contrary to the traditional view that ocean is the main moisture source. The possible reasons for this are that the oceanic moisture sources are too far away from YRV so the moisture cannot arrive directly, or these land regions are humid enough where ET amounts are actually close to or higher than that over ocean (not shown). This result is probably related to the spatial distribution of ET in MERRA, which is high over land compared to other global estimates [*Jiménez et al.*, 2011] and lower than other reanalyses over ocean but more realistic [*Bosilovich et al.*, 2011]. Biases in MERRA may also contribute to this; it is found that the reanalyses may tend to underestimate the lifetime of water vapor in the atmosphere [*Trenberth et al.*, 2011].

4. Variability and Implications for Rainfall Forecasts

[10] Figure 4 shows the relationships of local precipitation recycling with rainfall and ET over YRV during June–July based on pentad means. There is a very significant negative relationship between local recycling ratio and rainfall over YRV (Figure 4a). It means that when the YRV precipitation is higher (lower) there is a lower (higher) percentage of moisture from the local source. However, the absolute amount of local moisture contribution is generally higher for higher precipitation. Figures 4c and 4d further support the conclusion of Figure 4a by showing the composites of percentage moisture sources for high- and low-intensity rainfall events. High-intensity rainfall is associated with large percentage of moisture from remote sources, while the moisture for low-intensity rainfall is mainly from local evaporation. It appears that the recycling ratio is responding passively to the variation of rainfall, which is largely controlled by external factors. The correlation between total ET and rainfall over YRV is significantly negative (Figure 4b), indicating that the soil is very wet and ET is not constrained by surface wetness but by surface radiation. The lack of connection between total ET and its part that contributed to rainfall (Figure 4b) also implies the weak control of local surface condition on rainfall. This result is related to the choice of the region where moisture transport strongly affects rainfall (Figure 1). It is supported by some model simulations and analyses of observational based data [*Kim and Hong*, 2007; *Zhang et al.*, 2011; *Dirmeyer*, 2011], and is a feature over both YRV and its major water vapor transport pathways over land, so soil moisture is difficult to use as a direct factor for rainfall forecast. The above has shown the results from the rainy season (June–July); similar results are obtained for April–May and August–September except that the ET-rainfall relationship is weaker because of the changed rainfall and surface conditions. Completely different features are found over the Sahel (not shown), a semiarid region where soil moisture has a strong impact on ET and rainfall [*Taylor et al.*, 1997; *Taylor*, 2008; *Koster et al.*, 2004; *Dirmeyer*, 2011].

[11] Next, we look at the interannual variability of evaporative sources for YRV rainfall. An important question in

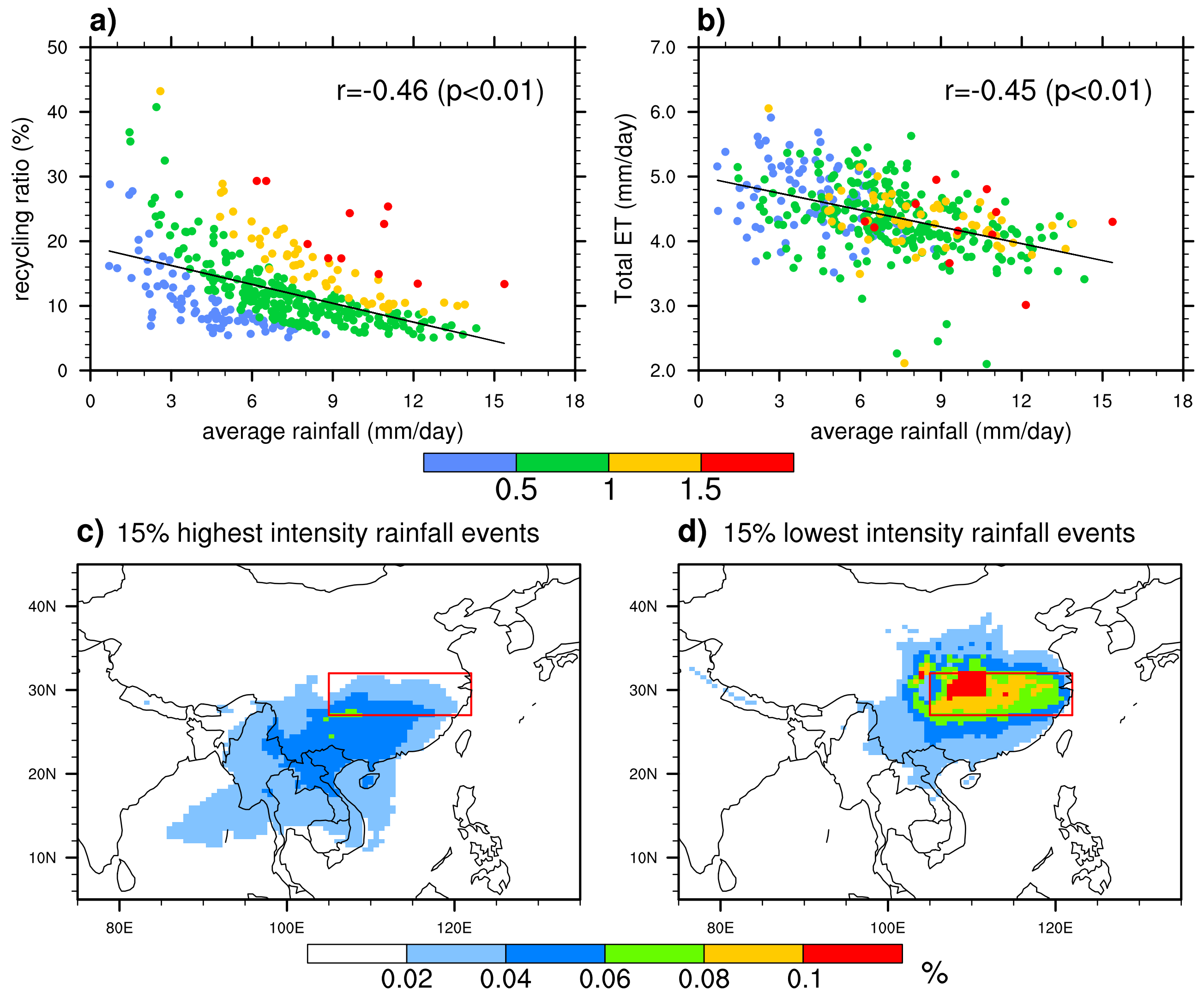

Figure 4. Scatterplots showing the dependence of (a) the YRV pentad recycling ratio and (b) the YRV pentad total ET on average rainfall during June–July (1979–2010). The colors of the dots show the evaporation from YRV that contributes to local rainfall (unit: mm/day). Linear regressions and correlations are also shown. Average percentages of the evaporative sources for (c) 15% highest intensity pentad precipitation events and (d) 15% lowest intensity pentad precipitation events aggregated independently for each grid point in the box (not including pentads and grid points with no precipitation).

the research of water vapor sources is where the evaporation is most important for precipitation in a certain region. This information may be helpful for precipitation forecasts. PCA is a useful tool to find the dominant spatial patterns and their temporal principal components (PCs). It emphasizes the consistent variability at large spatial scales so biases at small spatial scales have less impact. Figure 5 shows the first components (EOF1s) of interannual variability for the three periods. They explain about 25% of the interannual variance of evaporative moisture sources for each period. The pattern for April–May highlights the moisture sources over the South China Sea and South China. The pattern for June–July highlights the remote moisture sources from the Bay of Bengal, northern Indochina, and Southwest China, corresponding to the first branch of the moisture sources in Figure 2c. For August–September, the dominant pattern highlights moisture from South China, Indochina, and YRV. As the sum of the evaporative sources equals YRV precipitation, moisture from the highlighted evaporative sources is most important for the interannual variability of rainfall over YRV. This is confirmed by the very strong correlations between the time series of PC1s and YRV rainfall.

[12] Figure 6 shows the second components (EOF2s) of the PCA. Different from EOF1s, which mostly highlight nonlocal moisture sources, EOF2s show large contributions from YRV, tending to highlight local moisture recycling. Thus we compare the time series of YRV recycling ratio with those of PC2s (Figure 6). During June–July and August–September, the correlations between the recycling ratio and PC2 are very significant ($p < 0.01$). The correlation is weak during April–May, probably because it also highlights a large amount of moisture from nonlocal sources. The pattern for August–September shows an obvious typhoon path from the western Pacific to the lower reaches of YRV,

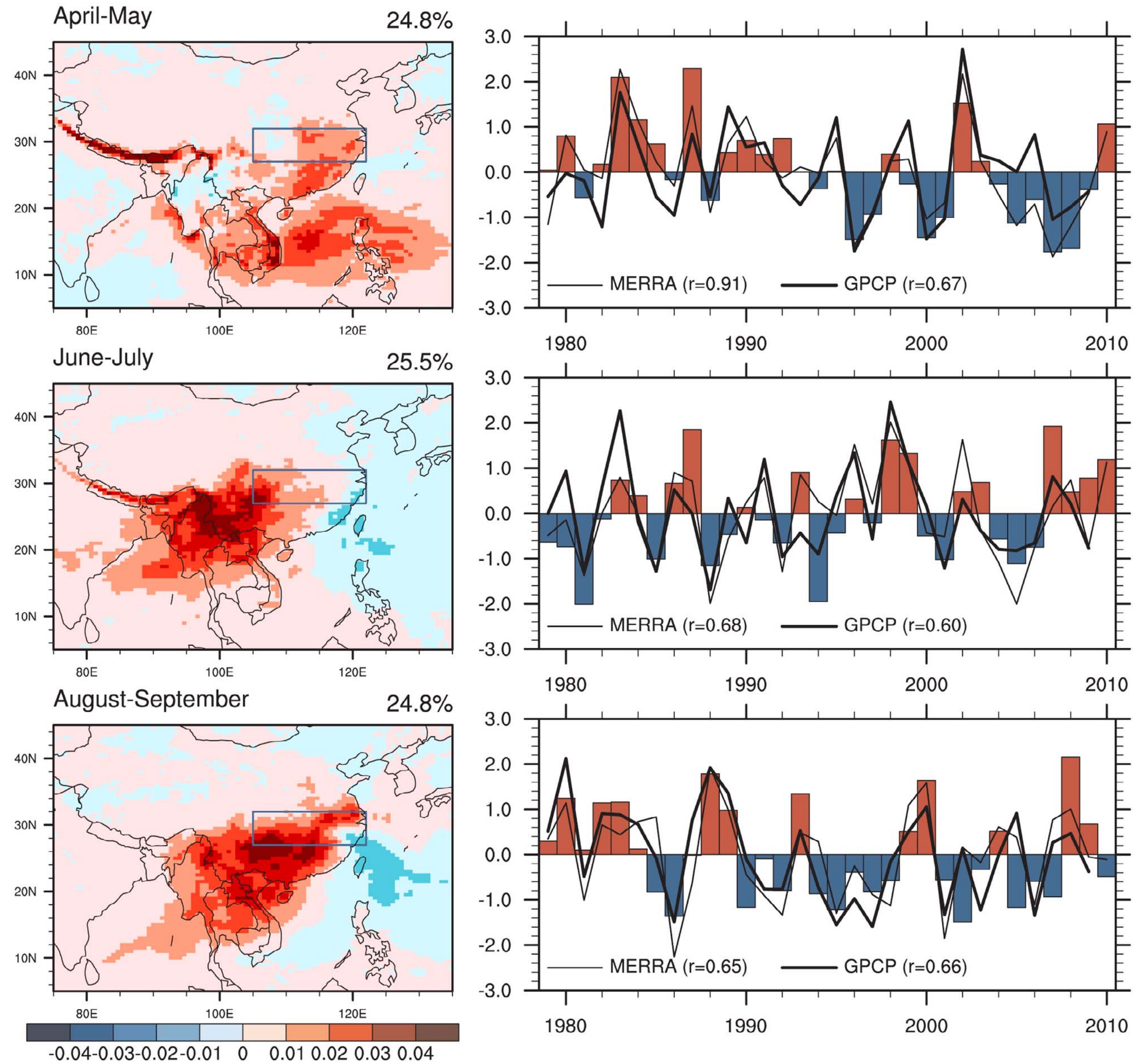

Figure 5. (left) The spatial distributions of the first EOFs and (right) their corresponding normalized principal component (PC) time series (bars) for the 1979–2010 interannual variations of the evaporative moisture sources for precipitation over YRV (blue box). (top) April–May, (middle) June–July, and (bottom) August–September averages. The EOFs are shown as the relative amplitude of moisture sources. Also shown with the PCs are the normalized interannual variations of average precipitation over YRV from MERRA and GPCP. Their correlation coefficients with corresponding PCs are shown, and all correlations are significant at the $p < 0.01$ level.

emphasizing the importance of typhoon on YRV rainfall. This is related to the fact that August–September is the peak season for typhoon impact on China [*Ren et al.*, 2002].

[13] The PC2 time series of June–July and August–September both show evident decadal variations from negative to positive values. Although the timing of this decadal change is consistent with the beginning of an observing system change (Advanced Microwave Sounding Unit (AMSU)), the effect of this observing system change is mainly more moisture and precipitation over tropical ocean [*Robertson et al.*, 2011; *Bosilovich et al.*, 2011] and MERRA does not show obvious differences in decadal precipitation variability from observations over YRV (Figure 5). We think these decadal changes in PCs and recycling ratio are probably related to the circulation changes that led to decreased rainfall over YRV after year 2000 [*Zhu et al.*, 2011] (note the negative correlation between rainfall and the recycling ratio shown in Figure 4). The increasing typhoon influence on YRV rainfall is supported by some recent studies [*Wu et al.*, 2005; *Tu et al.*, 2009], and there is a suggestion that it is related to global warming [*Wang et al.*, 2011].

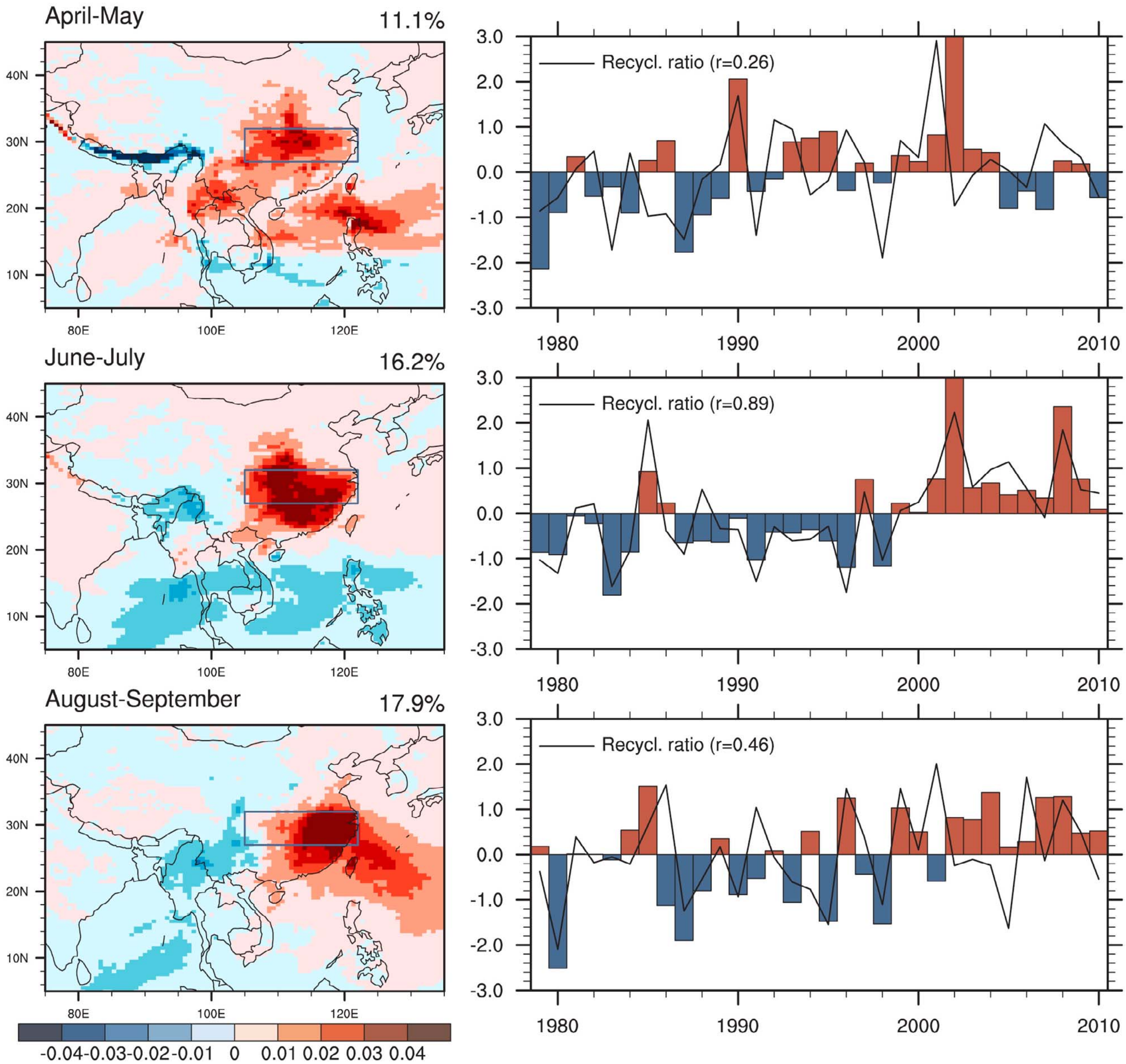

Figure 6. Same as Figure 5 but for the second EOFs and their corresponding PCs, and shown with the PC time series are the recycling ratios over YRV. Their correlation coefficients with corresponding PCs are shown.

[14] An interesting dipole pattern over the Bay of Bengal and western Pacific can be found in EOF1 during June–July and August–September (Figure 5) and in EOF2 during August–September (Figure 6). The moistures from the above two regions also show a seesaw relationship during April–September (Figure 3c). Moreover, *Zhang* [2001] found a positive interannual correlation between the zonal moisture fluxes over the Bay of Bengal and over the western tropical Pacific (opposite directions) during June–August. These results lead us to further investigate this problem. Figure 7 shows the monthly variation of the interannual correlation between moisture sources from the Bay of Bengal and from the western Pacific for YRV rainfall. Their correlation is significantly positive during the YRV cold season (November to April of next year) but decreases and becomes negative during the warm season, with a negative maximum in August. This shows why they have dipole patterns in the EOFs during August–September but not during April–May.

[15] The EOF1 (Figure 5) has shown the dominant evaporative sources for YRV precipitation. Can these moisture sources contribute to the prediction of YRV rainfall? We use another method to further examine this problem. The first step to identify a strong connection between precipitation in the destination region and its evaporative sources is to calculate their correlation coefficient (Figure 8, first row; the correlation squared is used to match the other two factors below, which are percentage rates). But a high correlation alone cannot guarantee an important water vapor source because some regions with high correlation contribute very

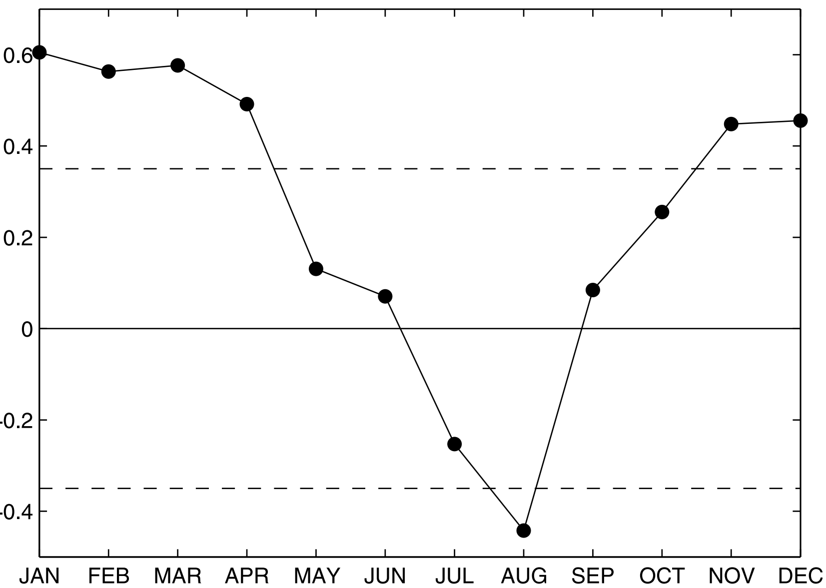

Figure 7. The monthly variation of the interannual correlation between moisture sources from the Bay of Bengal and from the western Pacific (defined in Figure 3a) for YRV precipitation. The horizontal dashed lines indicate the 95% confidence level.

little water vapor, and the high correlations could be caused by circulation patterns. On the other hand, the regions with large percentages of moisture contribution are more likely to have strong direct impact on the precipitation in the destination region. Therefore, the percentage contributions of the evaporation at each grid point to the total precipitation are another important factor to consider (Figure 8, second row; same as in Figure 2). The above two factors are enough to highlight the important water vapor source regions. However, from the perspective of prediction, the evaporative moisture from the source region that contributes to the precipitation must be a large fraction of the total evaporation in that region. Otherwise the information of evaporation in the source region is difficult to be used for precipitation prediction. Thus we further calculate the percentage of the total evaporation at each grid point that contributed to the precipitation (Figure 8, third row). By equally considering the three factors, we calculate their product (Figure 8, fourth row). By definition, the product highlights critical regions where evaporation may has the greatest impact on the interannual variation of YRV precipitation by directly providing moisture, and knowing the evaporation from these regions can potentially contribute to the prediction of YRV precipitation.

[16] In fact, the product of only the first two factors has a good correspondence to the EOF1 of evaporative source in Figure 5 because it considers both the consistent spatial variability (first factor) and amplitude (second factor). The third factor is not considered by PCA. Analysis shows that the products of two factors (not shown) and three factors have similar patterns, and they are very similar to the patterns of EOF1 (Figure 5). This provides an independent verification of PCA results.

[17] In Figure 8, the products of the three factors show most of the high values over local and surrounding land, which means the evaporation there may provide information for rainfall forecasts over YRV. However, the fraction of ET that contributes to YRV rainfall (third factor) is not high over these regions (<30%), and the ET there does not have a strong correlation with its part that contributes to YRV rainfall (Figure 4b). These factors limit the utility of land soil moisture or ET for rainfall forecasting over YRV, as shown by some modeling studies [*Kim and Hong*, 2007]. Thus, the prediction of YRV rainfall must rely on the information of large-scale circulation.

[18] It can be seen in Figure 8 that the correlations between YRV rainfall and its moisture sources (first factor) show very different patterns from those of the percentage contributions (second factor). Correlations with many oceanic sources are higher than those with the land sources and the products show significant values over some ocean regions, although the land sources are closer to YRV and contribute more moisture. This is probably because the ocean is the main originator of the large-scale monsoon flow that transports moisture to YRV while the land ET is affected by the complex land surface processes in addition to the oceanic forcing.

[19] Finally, a look at the composite difference between the wettest and driest cases sheds light on the factors causing the difference. Figure 9 shows the difference in evaporative sources, moisture fluxes, and SST between six wettest (1983, 1986, 1991, 1996, 1998, and 2002) and six driest (1981, 1985, 1988, 1992, 2001, 2005) rainy seasons (June–July) of YRV for the 32-year period. As MERRA is not completely consistent with the observation (GPCP) in interannual variability, we only chose the years in which they have consistent maximum/minimum values. The difference in evaporative sources is similar to EOF1 (Figure 5) or the product in Figure 8. The moisture flux difference is consistent with the pattern shown in Figure 1, confirming its dominant impact. The difference in SST shows an obvious El Niño-like pattern, consistent with previous studies [e.g., *Zhang et al.*, 1999; *Wang and Li*, 2004], and the weaker South Asian monsoon flow is probably related to this. The

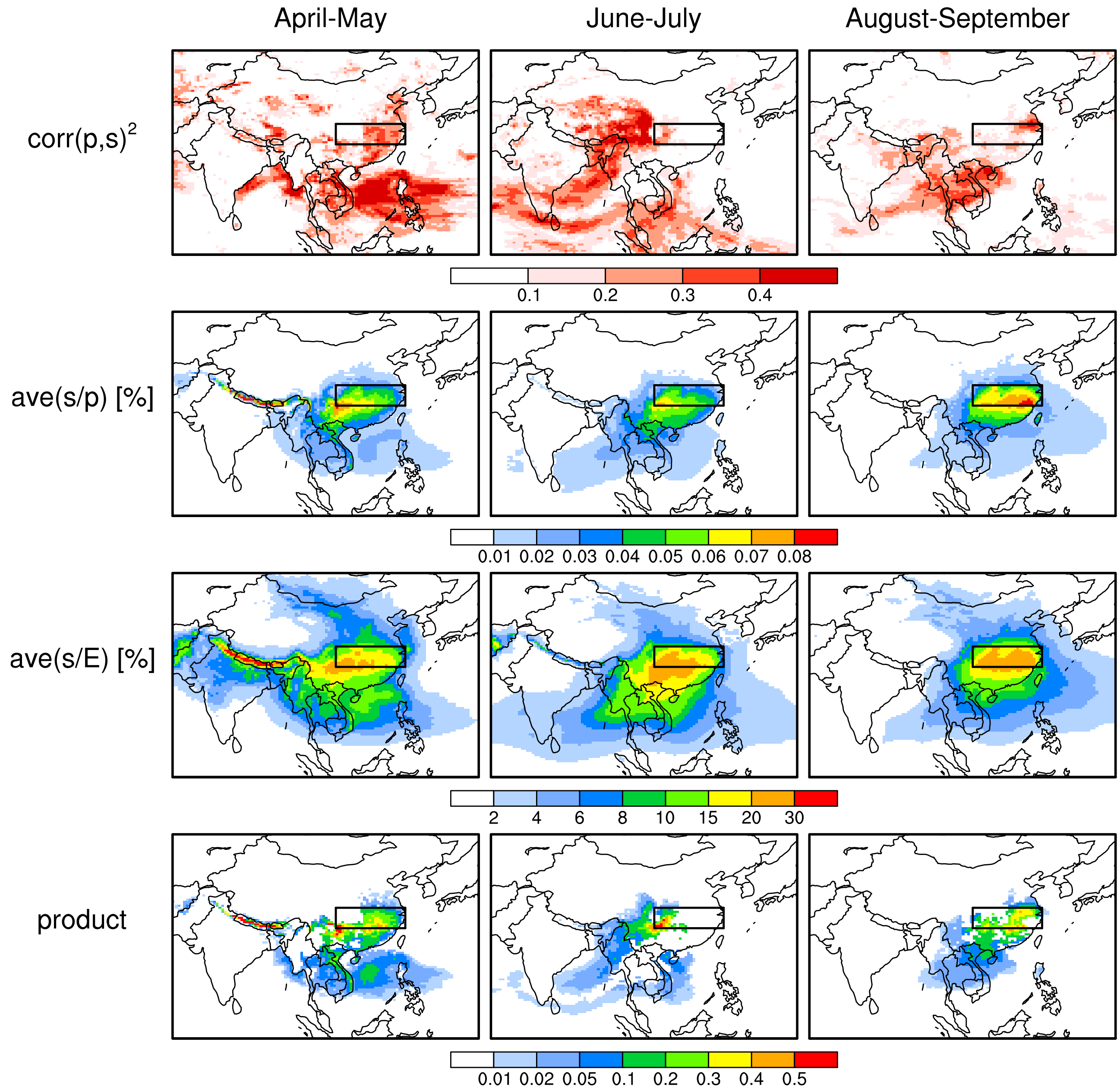

Figure 8. The first row shows interannual squared correlations between the total precipitation over YRV and its evaporative sources, the second row shows average percentages of evaporative source that contribute to the YRV precipitation, the third row shows fractions of total evaporation at each grid point that contribute to the precipitation over YRV, and the fourth row shows the product of the first three rows showing the critical evaporative sources for YRV precipitation. (left) April–May, (middle) June–July, and (right) August–September. Only the areas significant at the 95% level are shaded.

SST over the major oceanic moisture sources (the Bay of Bengal and South China Sea) is warmer, which may provide more evaporated moisture for YRV rainfall. But this effect of SST on YRV rainfall may be much weaker than its effect on the large-scale monsoon flow and moisture flux because a small amount of moisture is directly from ocean.

5. Summary

[20] The QIBT method is used to investigate the water vapor sources for YRV rainfall. The method tracks the evaporative sources for precipitation, which are difficult to obtain from moisture flux estimates. During the YRV wet season that we are investigating (April–September), the moisture sources for YRV rainfall show large seasonal variations, and their relative importance also change with time. The major paths for moisture transport to YRV are from the Bay of Bengal (southwest), the South China Sea (south), or the western Pacific (southeast), depending on time.

[21] The moisture from the Bay of Bengal and the western Pacific shows a seesaw relationship during the wet season, and has a negative interannual correlation during the warm

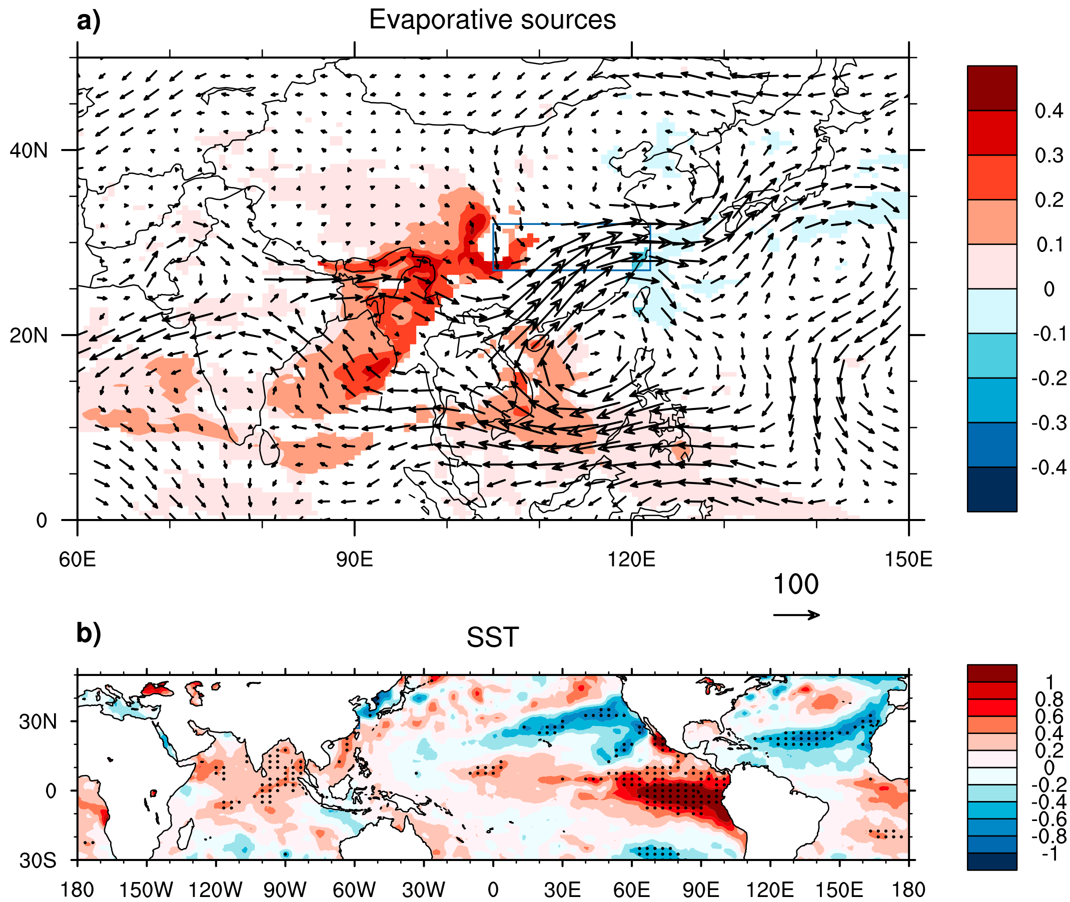

Figure 9. The composite differences in (a) evaporative sources for YRV rainfall (shading) and vertically integrated moisture fluxes (arrows) and (b) SST between the average of six wettest years and the average of six driest years over YRV during June–July. The shaded areas in Figure 9a and dotted areas in Figure 9b are significant at 90% confidence level, according to a bootstrap test of permuting the original time series for 10,000 times.

season (July–August) but a positive correlation during the cold season (October to April of next year). It is found that the most important moisture sources are mainly over the pathway(s) for moisture transport over land, but the ocean plays an important role in initiating the transport. PCA also reveals increased local recycling ratio and typhoon impact over YRV beginning around year 2000, which is consistent with some previous studies. Although the ocean is important for the moisture transport to YRV, the direct evaporative moisture sources are mainly over the local and surrounding land. Thus land-atmosphere interaction is an important issue affecting moisture transport. It is found that although the local ET of YRV accounts for about 10–15% of the moisture supplying rainfall, the local recycling of moisture is a passive response to the rainfall and large-scale circulation and contributes little to the interannual variability of YRV rainfall. Over YRV and its major moisture sources over land, the surface soil wetness does not have a strong control on ET and ET does not have a strong connection with its part that contributes to YRV rainfall. Therefore, the rainy season rainfall forecasts must rely on an accurate forecast of the large-scale circulation in which ocean plays an important role.

[22] This study demonstrates a gap between knowing the moisture sources for precipitation and using this information for precipitation forecast. For YRV, this information is not very useful. But it may be useful for other regions, like the Sahel. Using this information properly requires knowledge of land-atmosphere interaction and/or ocean-atmosphere interaction, depending on the sources of moisture. Moreover, for nonlocal moisture sources, the transport of moisture is usually controlled by the large-scale circulation, making the problem more complex. This study paves the way for studying nonlocal impact of surface ET on precipitation, and may contribute to the improvement of precipitation prediction.

[23] At last, this study is based on only one reanalysis data set. Although the results from other data sets may differ somewhat, we do not expect the results to differ significantly at the large scale. Preliminary comparisons with the results from NCEP-DOE reanalysis 2 [*Dirmeyer and Brubaker*, 2007] support this. In addition, the QIBT method, although has been used in several studies, has not been evaluated on its performance. Comparison of its results with those from the water vapor tracers in models is going on and a validation of the method will be provided.

[24] **Acknowledgments.** We thank the three reviewers for their constructive comments. The Goddard Earth Sciences (GES) Data and Information Services Center (DISC) are acknowledged by making the MERRA data online. This work was supported by grants from National Aeronautics and Space Administration (NNX09AI84G) of USA and National Basic Research Program of China (2012CB955604).

References

Adler, R. F., et al. (2003), The Version 2 Global Precipitation Climatology Project (GPCP) monthly precipitation analysis (1979-present), *J. Hydrometeorol.*, *4*, 1147–1167, doi:10.1175/1525-7541(2003)004<1147:TVGPCP>2.0.CO;2.

Bosilovich, M. G., and S. D. Schubert (2002), Water vapor tracers as diagnostics of the regional hydrologic cycle, *J. Hydrometeorol.*, *3*, 149–165, doi:10.1175/1525-7541(2002)003<0149:WVTADO>2.0.CO;2.

Bosilovich, M. G., F. R. Robertson, and J. Chen (2011), Global energy and water budgets in MERRA, *J. Clim.*, *24*, 5721–5739, doi:10.1175/2011JCLI4175.1.

Chen, J. L., and R. H. Huang (2008), Interannual and interdecadal variations of moisture transport by Asian summer monsoon and their association with droughts or floods in China [in Chinese], *Chin. J. Geophys.*, *51*, 352–359.

Ding, Y. H., and J. C. L. Chan (2005), The East Asian summer monsoon: An overview, *Meteorol. Atmos. Phys.*, *89*, 117–142, doi:10.1007/s00703-005-0125-z.

Ding, Y. H., Z. Wang, and Y. Sun (2008), Inter-decadal variation of the summer precipitation in East China and its association with decreasing Asian summer monsoon. Part I: Observed evidences, *Int. J. Climatol.*, *28*, 1139–1161, doi:10.1002/joc.1615.

Dirmeyer, P. A. (2011), The terrestrial segment of soil moisture–climate coupling, *Geophys. Res. Lett.*, *38*, L16702, doi:10.1029/2011GL048268.

Dirmeyer, P. A., and K. L. Brubaker (1999), Contrasting evaporative moisture sources during the drought of 1988 and the flood of 1993, *J. Geophys. Res.*, *104*, 19,383–19,397, doi:10.1029/1999JD900222.

Dirmeyer, P. A., and K. L. Brubaker (2007), Characterization of the global hydrologic cycle from a back-trajectory analysis of atmospheric water vapor, *J. Hydrometeorol.*, *8*, 20–37, doi:10.1175/JHM557.1.

Drumond, A., R. Nieto, and L. Gimeno (2011), A preliminary analysis of the sources of moisture for China and their variations during drier and wetter conditions in 2000–2004: A Lagrangian approach, *Clim. Res.*, *50*, 215–225, doi:10.3354/cr01043.

He, J., et al. (2007), Seasonal transition features of large-scale moisture transport in the Asian-Australian monsoon region, *Adv. Atmos. Sci.*, *24*, 1–14, doi:10.1007/s00376-007-0001-5.

Huang, R. H., Z. Z. Zhang, G. Huang, and B. H. Ren (1998), Characteristic of the water vapor transport in East Asian monsoon region and its difference from that in South Asian monsoon region in summer [in Chinese], *Chin. J. Atmos. Sci.*, *22*, 460–469.

Huang, R. H., G. Huang, and Z. G. Wei (2004), Climate variations of the summer monsoon over China, in *East Asian Monsoon*, edited by C.-P. Chang, pp. 213–268, World Sci., Singapore.

Jiménez, C., et al. (2011), Global intercomparison of 12 land surface heat flux estimates, *J. Geophys. Res.*, *116*, D02102, doi:10.1029/2010JD014545.

Kim, J.-E., and S.-Y. Hong (2007), Impact of soil moisture anomalies on summer rainfall over East Asia: A regional climate model study, *J. Clim.*, *20*, 5732–5743, doi:10.1175/2006JCLI1358.1.

Koster, R. D., et al. (2004), Regions of strong coupling between soil moisture and precipitation, *Science*, *305*, 1138–1140, doi:10.1126/science.1100217.

Numaguti, A. (1999), Origin and recycling processes of precipitating water over the Eurasian continent: Experiments using an atmospheric general circulation model, *J. Geophys. Res.*, *104*(D2), 1957–1972, doi:10.1029/1998JD200026.

Ren, F., B. Gleason, and D. Easterling (2002), Typhoon impacts on China's precipitation during 1957–1996, *Adv. Atmos. Sci.*, *19*, 943–952, doi:10.1007/s00376-002-0057-1.

Rienecker, M. M., et al. (2011), MERRA: NASA's Modern-Era Retrospective Analysis for Research and Applications, *J. Clim.*, *24*, 3624–3648, doi:10.1175/JCLI-D-11-00015.1.

Robertson, F. R., M. G. Bosilovich, J. Chen, and T. L. Miller (2011), The effect of satellite observing system changes on MERRA water and energy fluxes, *J. Clim.*, *24*, 5197–5217, doi:10.1175/2011JCLI4227.1.

Simmonds, I., D. Bi, and P. Hope (1999), Atmospheric water vapor flux and its association with rainfall over China in summer, *J. Clim.*, *12*, 1353–1367, doi:10.1175/1520-0442(1999)012<1353:AWVFAI>2.0.CO;2.

Sodemann, H., C. Schwierz, and H. Wernli (2008), Interannual variability of Greenland winter precipitation sources: Lagrangian moisture diagnostic and North Atlantic Oscillation influence, *J. Geophys. Res.*, *113*, D03107, doi:10.1029/2007JD008503.

Stohl, A., and P. James (2004), A Lagrangian analysis of the atmospheric branch of the global water cycle. Part I: Method description, validation, and demonstration for the August 2002 flooding in central Europe, *J. Hydrometeorol.*, *5*, 656–678, doi:10.1175/1525-7541(2004)005<0656:ALAOTA>2.0.CO;2.

Taylor, C. M. (2008), Intraseasonal land–atmosphere coupling in the West African monsoon, *J. Clim.*, *21*, 6636–6648, doi:10.1175/2008JCLI2475.1.

Taylor, C. M., F. Saïd, and T. Lebel (1997), Interactions between the land surface and mesoscale rainfall variability during HAPEX-Sahel, *Mon. Weather Rev.*, *125*, 2211–2227, doi:10.1175/1520-0493(1997)125<2211:IBTLSA>2.0.CO;2.

Trenberth, K., J. T. Fasullo, and J. Mackaro (2011), Atmospheric moisture transports from ocean to land and global energy flows in reanalyses, *J. Clim.*, *24*, 4907–4924, doi:10.1175/2011JCLI4171.1.

Tu, J.-Y., C. Chou, and P.-S. Chu (2009), The abrupt shift of typhoon activity in the vicinity of Taiwan and its association with western North Pacific–East Asian climate change, *J. Clim.*, *22*, 3617–3628, doi:10.1175/2009JCLI2411.1.

Wang, B., and T. Li (2004), East Asian monsoon-ENSO interactions, in *East Asian Monsoon*, edited by C.-P. Chang, pp. 177–212, World Sci., Singapore.

Wang, R., L. Wu, and C. Wang (2011), Typhoon track changes associated with global warming, *J. Clim.*, *24*, 3748–3752.

Wu, L., B. Wang, and S. Geng (2005), Growing typhoon influence on east Asia, *Geophys. Res. Lett.*, *32*, L18703, doi:10.1029/2005GL022937.

Xie, P., and P. A. Arkin (1997), Global precipitation: A 17-year monthly analysis based on gauge observations, satellite estimates, and numerical model outputs, *Bull. Am. Meteorol. Soc.*, *78*, 2539–2558, doi:10.1175/1520-0477(1997)078<2539:GPAYMA>2.0.CO;2.

Xie, P., J. E. Janowiak, P. A. Arkin, R. Adler, A. Gruber, R. Ferraro, G. J. Huffman, and S. Curtis (2003), GPCP pentad precipitation analyses: An experimental dataset based on gauge observations and satellite estimates, *J. Clim.*, *16*, 2197–2214, doi:10.1175/2769.1.

Xu, X. D., X. Y. Shi, Y. Q. Wang, S. Q. Peng, and X. H. Shi (2008), Data analysis and numerical simulation of moisture source and transport associated with summer precipitation in the Yangtze River Valley over China, *Meteorol. Atmos. Phys.*, *100*, 217–231, doi:10.1007/s00703-008-0305-8.

Zhang, J., L. Wu, and W. Dong (2011), Land-atmosphere coupling and summer climate variability over East Asia, *J. Geophys. Res.*, *116*, D05117, doi:10.1029/2010JD014714.

Zhang, R. (2001), Relations of water vapor transport from Indian monsoon with that over East Asia and the summer rainfall in China, *Adv. Atmos. Sci.*, *18*, 1005–1017.

Zhang, R., A. Sumi, and M. Kimoto (1999), A diagnostic study of the impact of El Niño on the precipitation in China, *Adv. Atmos. Sci.*, *16*, 229–241, doi:10.1007/BF02973084.

Zhao, R. X., G. X. Wu, and H. Zhang (2008), Seasonal characteristic and interannual variability of the atmospheric hydrological cycle in the Yangtze River basin during the summer monsoon period [in Chinese], *Chin. J. Geophys.*, *51*, 1670–1681.

Zhou, T.-J., and R.-C. Yu (2005), Atmospheric water vapor transport associated with typical anomalous summer rainfall patterns in China, *J. Geophys. Res.*, *110*, D08104, doi:10.1029/2004JD005413.

Zhou, X. X., Y. H. Ding, and P. X. Wang (2008), Moisture transport in the Asian summer monsoon region and its relationship with summer precipitation in China, *Acta Meteorol. Sinica*, *24*(1), 31–42.

Zhu, Y., H. Wang, W. Zhou, and J. Ma (2011), Recent changes in the summer precipitation pattern in East China and the background circulation, *Clim. Dyn.*, *36*, 1463–1473, doi:10.1007/s00382-010-0852-9.

M. G. Bosilovich, Global Modeling and Assimilation Office, NASA Goddard Space Flight Center, Greenbelt, MD 20771, USA.

P. A. Dirmeyer and J. Wei, Center for Ocean-Land-Atmosphere Studies, Institute of Global Environment and Society, Calverton, MD 20705, USA. (jianfeng@cola.iges.org)

R. Wu, Institute of Space and Earth Information Science, Chinese University of Hong Kong, Fok Ying Tung Remote Sensing Science Building, Shatin, Hong Kong.